

Power-Law Inflation Survives Observational Constraints

Yao Yu,^{1,2,*} Wen-Zhang Feng,¹ Hong-Song Xie,¹ Han Zhang,³ and Bai-Cian Ke^{3,†}

¹*Chongqing University of Posts & Telecommunications, Chongqing, 400065, China*

²*Department of Physics and Chongqing Key Laboratory for Strongly Coupled Physics,
Chongqing University, Chongqing 401331, People's Republic of China*

³*School of Physics, Zhengzhou University, Zhengzhou, Henan 450001, China*

Abstract

Power-law inflation has stood as a classical model in inflationary cosmology since the early 1980s, prized for its exact analytical solutions and ability to naturally resolve the Big Bang theory's horizon and flatness problems through exponential expansion. However, its simplest form appears incompatible with modern precision observations, motivating increasingly complex alternatives. In this work, we demonstrate how previous predictions with power-law inflation considered only a particular solution of the field equations, and derive the complete set of general analytical solutions that satisfy current theoretical and observational constraints. This finding revitalizes power-law inflation as a viable framework, offering new possibilities for cosmological model-building while preserving its original mathematical elegance.

* Corresponding author: yuyao@cqupt.edu.cn

† Corresponding author: baiciank@ihep.ac.cn

Inflation is the period of exponential expansion in the early Universe and decides the initial conditions for the subsequent hot Big Bang era [1]. Inflation explains why the universe appears spatially flat, homogeneous, and isotropic on large scales, features that are difficult to account for within the Big Bang theory alone [2, 3]. Moreover, inflation resolves the horizon problem by allowing regions currently far apart to have once been in causal contact, thus explaining the uniform temperature observed in the cosmic microwave background (CMB). It can also account for the origin of the cosmological fluctuations and predicts a nearly scale-invariant power spectrum for the fluctuations [4, 5].

Numerous different scenarios for inflation have been developed to describe observational data, particularly the scalar spectral index n_s and tensor-to-scalar ratio r of primordial gravity waves. These scenarios typically involve nonlinear ordinary differential equations, forcing most relevant investigations to rely on numerical calculations with simplifying approximations, such as the slow-roll approximation. A remarkable exception was power-law inflation, developed by Lucchin and Matarrese in the early 1980s [6–10], which provided an elegant cosmological scenario with exact analytical solutions to the inflationary field equations. Its exponential potential ($V(\phi) \propto e^{-\lambda\phi}$) yielded power-law expansion ($a(t) \propto t^p$) without requiring the slow-roll approximation [11, 12]. This scenario’s mathematical simplicity enabled exact computation of primordial perturbations while naturally solving the Big Bang theory’s horizon and flatness problems through prolonged expansion (≥ 60 e-foldings). Regrettably, this theoretically elegant model has been effectively excluded by the latest CMB measurements of n_s and r , diminishing its role in recent inflationary studies and relegating it to a pedagogical tool with analytically solvable solutions.

Previous calculations with power-law inflation, however, considered only a particular solution, not the complete set of general solutions. This work introduces a transform of the inflationary field equations into Abel’s equation of the first kind [13, 14]. The exponential form of the power-law potential renders this equation analytically solvable, allowing us to obtain the general solutions. We demonstrate that these solutions can satisfy both theoretical requirements and current observational constraints, thereby restoring the viability of power-law inflation as a compelling cosmological scenario.

In the flat Friedmann-Lemaître-Robertson-Walker metric, the canonical homogeneous

inflaton field ϕ obeys the Klein-Gordon equation of motion:

$$\ddot{\phi} + 3H\dot{\phi} + \frac{dV}{d\phi} = 0, \quad (1)$$

where overdots denote time t derivatives, $V(\phi)$ is the inflationary potential, $H \equiv \dot{a}/a$ is the Hubble parameter, and a is the scale factor. During inflation when the Universe is dominated by the inflaton field, the Friedmann equation

$$H^2 = \frac{1}{3M_{\text{pl}}^2} \left(\frac{1}{2}\dot{\phi}^2 + V(\phi) \right) \quad (2)$$

couple the Hubble parameter to the inflaton's kinetic and potential energy, with $M_{\text{pl}} \equiv \frac{1}{\sqrt{8\pi G}}$ the reduced Planck mass. The dynamical equation for cosmic expansion is derived by combining Eqs. (1) and (2) and using the identity $\ddot{\phi} = \frac{d\dot{\phi}}{d\phi}\dot{\phi}$, written as

$$\frac{d\dot{\phi}}{d\phi}\dot{\phi} + 3\sqrt{\frac{1}{3M_{\text{pl}}^2} \left(\frac{1}{2}\dot{\phi}^2 + V(\phi) \right)}\dot{\phi} + \frac{dV}{d\phi} = 0. \quad (3)$$

The above equation constitutes a first-order nonlinear ordinary differential equation for $\dot{\phi}(\phi)$. A strategic variable transformation could convert the equation into a form better suited for analytical solutions. This transformation proceeds through the following three steps:

Step 1: Equation (3) is rewritten as

$$d \left[\sqrt{\frac{1}{2}\dot{\phi}^2 + V(\phi)} \right] + \frac{\sqrt{3}}{2M_{\text{pl}}}\dot{\phi}d\phi = 0. \quad (4)$$

Step 2: Applying the substitution $V(\phi) = g^2(\phi)$, with $\sqrt{\frac{1}{2}\dot{\phi}^2 + g^2(\phi)} = g(\phi) \cosh u(\phi)$ and $\dot{\phi} = \sqrt{2}g(\phi) \sinh u(\phi)$, transforms Eq. (4) into

$$\frac{du(\phi)}{d\phi} + \frac{d \ln g(\phi)}{d\phi} \coth u(\phi) + \frac{\sqrt{6}}{2M_{\text{pl}}} = 0. \quad (5)$$

Step 3: The final substitution

$$y(\phi) = \coth u(\phi) = \frac{\sqrt{\dot{\phi}^2 + 2V(\phi)}}{\dot{\phi}}, (|y| > 1) \quad (6)$$

yields

$$\frac{dy}{d\phi} = (y^2 - 1) \left(\frac{y}{2} \frac{d \ln V}{d\phi} + \frac{\sqrt{6}}{2M_{\text{pl}}} \right). \quad (7)$$

This equation is known as the *Abel equation of the first kind*, $dy/d\phi = f_3(\phi)y^3 + f_2(\phi)y^2 + f_1(\phi)y + f_0(\phi)$, where here $f_3(\phi) = -f_1(\phi) = \frac{1}{2} \frac{d \ln V(\phi)}{d\phi}$ and $f_2(\phi) = -f_0(\phi) = \frac{\sqrt{6}}{2M_{\text{pl}}}$. Similar approaches have been utilized in Ref. [15, 16].

For the power-law inflation potential $V = V_0 \exp(-\lambda\phi/M_{\text{pl}})$, Eq. (7) can be solved via separation of variables. It is convenient to introduce the variable ω defined by $\omega = \sqrt{3}/y$. The general exact solution is then given by

$$\left| \sqrt{3} - \omega \right|^{\frac{\lambda}{\lambda - \sqrt{6}}} \times \left| \sqrt{3} + \omega \right|^{\frac{\lambda}{\lambda + \sqrt{6}}} \times \left| \omega - \frac{\lambda}{\sqrt{2}} \right|^{\frac{2\lambda^2}{6 - \lambda^2}} = CV, \quad (8)$$

where λ is a dimensionless parameter and $C \geq 0$ is an integration constant. A similar result to the above expression was also obtained in Ref. [17] based on a different method. Note that ω^2 corresponds to the first Hubble flow parameter [18, 19]. Using Eqs. 2 and 3, one can express it as

$$\omega^2 = -\frac{\dot{H}}{H^2} = 1 - \frac{a}{\dot{a}^2} \ddot{a}, \quad (9)$$

which confirms that ω^2 coincides with the first Hubble flow parameter. The inflationary condition $\ddot{a} > 0$ is therefore equivalent to $\omega^2 < 1$, providing a clear physical interpretation of ω as a parameter indicating whether the universe is undergoing inflation. The previously studied exact solutions correspond to the special case $C = 0$ with $\omega = \lambda/\sqrt{2}$, for which the first Hubble flow parameter is constant. However, these $C = 0$ solutions are ruled out by Planck 2018 data ($n_s = 0.9649 \pm 0.0042$ [20]) and a combination of BICEP/Keck 2018 and Planck PR4 data ($r < 0.032$ at 95% C.L. [21–23]).

Our work therefore focuses on the case $C > 0$ to derive general solutions that are consistent with current observational constraints. The time derivative of the scalar field can be obtained using Eq. (6) as explicit functions of ω

$$\dot{\phi} = \omega \sqrt{\frac{2V}{3 - \omega^2}}. \quad (10)$$

Combining this with the Friedmann equation (Eq. (2)) yields the Hubble parameter

$$H = \frac{1}{M_{\text{pl}} \sqrt{\frac{V}{3 - \omega^2}}}. \quad (11)$$

For $C > 0$, substitution of the general solution from Eq. (8) gives $\dot{\phi}$ and H as

$$\begin{aligned} \dot{\phi} &= \sqrt{\frac{2}{C}} \omega \left| \sqrt{3} - \omega \right|^{\frac{\sqrt{6}}{2(\lambda - \sqrt{6})}} \times \left| \sqrt{3} + \omega \right|^{-\frac{\sqrt{6}}{2(\lambda + \sqrt{6})}} \times \left| \omega - \frac{\lambda}{\sqrt{2}} \right|^{\frac{\lambda^2}{6 - \lambda^2}}, \\ H &= \frac{1}{\sqrt{C} M_{\text{pl}}} \left| \sqrt{3} - \omega \right|^{\frac{\sqrt{6}}{2(\lambda - \sqrt{6})}} \times \left| \sqrt{3} + \omega \right|^{-\frac{\sqrt{6}}{2(\lambda + \sqrt{6})}} \times \left| \omega - \frac{\lambda}{\sqrt{2}} \right|^{\frac{\lambda^2}{6 - \lambda^2}}. \end{aligned} \quad (12)$$

Furthermore, Eq. (7) can be reformulated to express the evolution of ω with the field

$$\frac{d\omega}{d\phi} = -\frac{\sqrt{2}}{2M_{\text{pl}}}\frac{1}{\omega}(3-\omega^2)\left(\omega - \frac{\lambda}{\sqrt{2}}\right). \quad (13)$$

Combining the expression of $\dot{\phi}$ in Eq. (12), the time derivative of ω is given by

$$\dot{\omega} = \frac{d\omega}{d\phi}\dot{\phi} = \frac{1}{\sqrt{C}M_{\text{pl}}}\left(\sqrt{3}-\omega\right)^{\frac{\sqrt{6}}{2}\frac{1}{\lambda-\sqrt{6}}+1}\left(\sqrt{3}+\omega\right)^{-\frac{\sqrt{6}}{2}\frac{1}{\lambda+\sqrt{6}}+1}\left(\frac{\lambda}{\sqrt{2}}-\omega\right)\left|\omega - \frac{\lambda}{\sqrt{2}}\right|^{\frac{\lambda^2}{6-\lambda^2}} \quad (14)$$

Solving the above equation yields the explicit relation of ω and t

$$t = t_0 + \frac{c_0}{M_{\text{pl}}}\left|\frac{\lambda}{\sqrt{2}} - \omega\right|^{-\frac{\lambda^2}{6-\lambda^2}} \times F_1\left(-\frac{\lambda^2}{6-\lambda^2}; 1 - \frac{1}{2}\frac{\sqrt{6}}{\sqrt{6}-\lambda}, 1 - \frac{1}{2}\frac{\sqrt{6}}{\sqrt{6}+\lambda}; 1 - \frac{\lambda^2}{6-\lambda^2}; \frac{\omega - \frac{\lambda}{\sqrt{2}}}{\sqrt{3} - \frac{\lambda}{\sqrt{2}}}, -\frac{\omega - \frac{\lambda}{\sqrt{2}}}{\sqrt{3} + \frac{\lambda}{\sqrt{2}}}\right) \quad (15)$$

where

$$c_0 = \sqrt{C}M_{\text{pl}}^2\frac{6-\lambda^2}{\lambda^2}\left(\sqrt{3}-\frac{\lambda}{\sqrt{2}}\right)^{-\frac{\sqrt{6}}{2}\frac{1}{\lambda-\sqrt{6}}-1}\left(\sqrt{3}+\frac{\lambda}{\sqrt{2}}\right)^{\frac{\sqrt{6}}{2}\frac{1}{\lambda+\sqrt{6}}-1} \quad (16)$$

and $F_1(a; b_1, b_2; c; x, y)$ denotes the Appell hypergeometric function of the first kind [24, 25], and t_0 is an integration constant. Accordingly, the dynamical behavior of the field $\phi(t)$ in time t is derived in the parametric form of Eq. (15) and the following equation, which is obtained from Eq. (8)

$$\phi = \frac{M_{\text{pl}}}{\lambda}\left[\frac{\lambda}{\sqrt{6}-\lambda}\ln|\sqrt{3}-\omega| - \frac{\lambda}{\sqrt{6}+\lambda}\ln|\sqrt{3}+\omega| - 2\frac{\lambda^2}{6-\lambda^2}\ln\left|\frac{\lambda}{\sqrt{2}}-\omega\right| + \ln(CV_0)\right]. \quad (17)$$

For completeness, we also analyze the $C = 0$ case to provide a comprehensive theoretical comparison. In this limit, ω is a constant, $\omega = \frac{\lambda}{\sqrt{2}}$, contrasting with the time-dependent behavior found for $C > 0$. Equations (10) and (11) yield the analytical form the time derivative of the scalar field and the Hubble parameter as

$$\begin{aligned} \dot{\phi} &= \lambda\sqrt{\frac{2V_0}{6-\lambda^2}}\exp\left(-\frac{\lambda}{2}\frac{\phi}{M_{\text{pl}}}\right), \\ H &= \frac{1}{M_{\text{pl}}}\sqrt{\frac{2V_0}{6-\lambda^2}} \end{aligned} \quad (18)$$

Consequently, the dynamical behavior of the field $\phi(t)$ in time t is given by

$$\phi = \frac{2M_{\text{pl}}}{\lambda}\ln\left[\frac{\lambda^2}{2M_{\text{pl}}}\sqrt{\frac{2V_0}{6-\lambda^2}}\right] + \frac{2M_{\text{pl}}}{\lambda}\ln[t + t_1], \quad (19)$$

where t_1 is an integration constant. The $C = 0$ results cannot be obtained by taking the $C \rightarrow 0$ limit of the $C > 0$ solutions, as this leads to an indeterminate $0/0$ form. This reveals an intrinsic analytic discontinuity; the analytic expression valid for $C > 0$ cannot be continuously extended to $C = 0$. Nevertheless, the $C = 0$ case remains structurally connected to the $C > 0$ case and should be interpreted as its non-smooth counterpart rather than as an entirely independent solution.

A complete understanding of the inflaton's behavior requires analysis of several key features: stability conditions (if an attractor), the number of e-foldings (typically $\gtrsim 60$ for successful inflation), super-Hubble evolution of perturbations, and the observable spectra (the scalar spectral index n_s and tensor-to-scalar ratio r). These features are now examined. This work concentrates on $|\lambda| < \sqrt{6}$ for clarity, a range that will later be shown to align with current observational constraints. The stability conditions are analyzed by assuming ϕ_c is a stable fixed point, a special type of an attractor, which satisfies

$$\dot{\phi}|_{\phi=\phi_c} = 0, \quad \left. \frac{d\dot{\phi}}{d\phi} \right|_{\phi=\phi_c} < 0. \quad (20)$$

The explicit expression for $\dot{\phi}$ in Eq. (12) is used to identify candidate fixed points. Their stability is then determined by evaluating the sign of the derivative $\frac{d\dot{\phi}}{d\phi}$ at these points. The derivative $\frac{d\dot{\phi}}{d\phi}$ is computed via the chain rule, $\frac{d\dot{\phi}}{d\phi} = \frac{d\dot{\phi}}{d\omega} \frac{d\omega}{d\phi}$, using Eq. (12) for $\dot{\phi}$ and Eq. (13) for $\frac{d\omega}{d\phi}$. The explicit form of $\frac{d\dot{\phi}}{d\phi}$ is derived to be

$$\frac{d\dot{\phi}}{d\phi} = \frac{d\dot{\phi}}{d\omega} \frac{d\omega}{d\phi} = \dot{\phi} \frac{d\omega}{d\phi} \left[\frac{1}{\omega} + 6 \frac{\frac{\lambda}{\sqrt{2}} + \omega}{(6 - \lambda^2)(3 - \omega^2)} + \frac{\lambda^2}{6 - \lambda^2} \frac{1}{\omega - \frac{\lambda}{\sqrt{2}}} \right]. \quad (21)$$

Distinct attractor behaviors emerge for different λ regimes, illustrated in Fig. 1:

- $0 < \lambda < \sqrt{6}$: When $\omega < 0$, $\omega \rightarrow 0$ (semi-stable fixed point), when $\omega > 0$, $\omega \rightarrow \lambda/\sqrt{2}$ (stable fixed point)
- $-\sqrt{6} < \lambda < 0$: When $\omega > 0$, $\omega \rightarrow 0$ (semi-stable fixed point), when $\omega < 0$, $\omega \rightarrow \lambda/\sqrt{2}$ (stable fixed point)
- $\lambda > \sqrt{6}$: When $\omega < 0$, $\omega \rightarrow 0$ (semi-stable fixed point); when $\omega > 0$, $\omega \rightarrow \sqrt{3}$ (stable fixed point).
- $\lambda < -\sqrt{6}$: When $\omega > 0$, $\omega \rightarrow 0$ (semi-stable fixed point); when $\omega < 0$, $\omega \rightarrow -\sqrt{3}$ (stable fixed point).

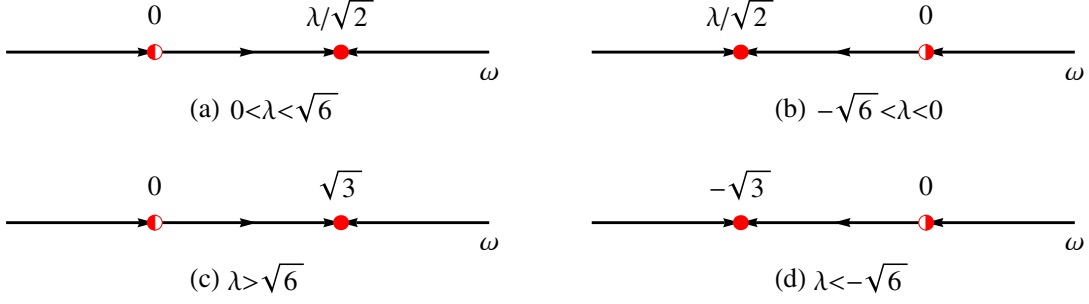


FIG. 1. Attractor behaviors for various values of λ

The limiting behavior of $\frac{d\phi}{d\omega}$ as $\omega \rightarrow 0$ are considered from both $\omega > 0$ and $\omega < 0$ directions, since $\frac{d\phi}{d\omega}$ exhibits a singularity at $\omega = 0$. For instance, when $0 < \lambda < \sqrt{6}$, only trajectories with $\omega > 0$ lies in the observationally allowed region; in this physical regime, the semi-stable point behaves as *repelling*, although mathematically it would become *attracting* for $\omega < 0$, a region not physically relevant. Once the value of ω is specified, the corresponding value of $\phi(\omega)$ in Eqs. (8) or (17) can be determined. For $0 < \lambda < \sqrt{6}$, as $\omega \rightarrow \lambda/\sqrt{2}$, the potential V approaches zero, corresponding to $\phi_c \rightarrow +\infty$. In contrast, for $-\sqrt{6} < \lambda < 0$, $\phi_c \rightarrow -\infty$.

The e-folding number N quantifies the exponential growth of the scale factor $a(t)$ of the universe and the Hubble parameter $H = \dot{a}/a$ represents the instantaneous expansion rate of the universe. For inflation from starting time t_i to ending t_e , N for the $C > 0$ case is given by

$$N \equiv \ln \frac{a(t_e)}{a(t_i)} = \int_{t_i}^{t_e} H dt = \int_{\omega_i}^{\omega_e} \frac{H}{\dot{\phi}} \frac{d\phi}{d\omega} d\omega = \int_{\omega_i}^{\omega_e} \frac{d\omega}{(\omega^2 - 3) \left(\omega - \frac{\lambda}{\sqrt{2}} \right)}. \quad (22)$$

Then one has

$$N = \frac{\sqrt{6}\lambda}{36 - 6\lambda^2} \ln \frac{\sqrt{3} - \omega}{\sqrt{3} + \omega} + \frac{1}{6 - \lambda^2} \ln \frac{3 - \omega^2}{\left(\omega - \frac{\lambda}{\sqrt{2}} \right)^2} \Big|_{\omega_i}^{\omega_e}. \quad (23)$$

Consequently, the scale factor's evolution $a(t)$ follows the parametric form of Eq. (15) with

$$a = a_0 \left| \sqrt{3} - \omega \right|^{\frac{\sqrt{6}}{6(\sqrt{6}-\lambda)}} \times \left| \sqrt{3} + \omega \right|^{\frac{\sqrt{6}}{6(\sqrt{6}+\lambda)}} \times \left| \omega - \frac{\lambda}{\sqrt{2}} \right|^{-\frac{2}{6-\lambda^2}}. \quad (24)$$

As for $C = 0$, the e-folding number is

$$N \equiv \ln \frac{a(t_e)}{a(t_i)} = \int_{t_i}^{t_e} H dt = \int_{\phi_i}^{\phi_e} \frac{H}{\dot{\phi}} d\phi = \frac{1}{\lambda M_{\text{pl}}} (\phi_e - \phi_i). \quad (25)$$

Combining this with Eq. (19), the scale factor is written as

$$a(t) = a_1(t + t_1)^{\frac{2}{\lambda^2}}, \quad (26)$$

where a_1 is an integration constant. According to Eqs. (24) and (26), this model does not naturally provide a graceful exit from inflation, and an additional mechanism to end inflation must be introduced. It is common in the literature to treat the inflationary phase and its termination separately, because observational constraints mainly depend on the dynamics during inflation rather than the specifics of its ending. For instance, constant-roll inflation [26, 27] likewise lack a built-in exit mechanism and require an additional scheme, such as that described in Ref. [28], to terminate inflation.

The analytical solutions for $\omega(t)$, $\phi(t)$, and $a(t)$ are presented in Fig. 2, which compares the $C > 0$ and $C = 0$ results. While the corresponding evolutions are nearly identical across most of the inflationary history, they diverge at the initial stage, following distinct trajectories before converging. During the approach to the stable point, $\omega(t)$ tends to a constant, $\phi(t)$ increases, and $a(t)$ exhibits convex growth, signaling an accelerated expansion. As will be shown, the early-time trajectories along which the solutions approach their stable points are critical, leading to significantly different cosmological observables, such as the scalar spectral index n_s and the tensor-to-scalar ratio r .

The comoving curvature perturbation ζ is the key variable that describes how scalar field fluctuations influence the geometry of spacetime. Through appropriate gauge choices and variable redefinitions, the system of perturbations can be reduced to a single dynamical degree of freedom, $\nu = z\zeta$ and $z = a\dot{\phi}/H$. The variable ν can be reconstructed via the Fourier transform,

$$\nu(\tau, \vec{x}) = \int \frac{d^3k}{(2\pi)^3} \nu_k(\tau) e^{i\vec{k}\cdot\vec{x}}, \quad (27)$$

Here, $\tau \equiv \int a^{-1} dt$ is the conformal time and ν_k is the canonically normalized, gauge-invariant scalar perturbation in Fourier space. The evolution of ν_k is governed by the Mukhanov-Sasaki equation [29, 30]

$$\nu_k'' + \left(k^2 - \frac{z''}{z} \right) \nu_k = 0, \quad (28)$$

where a prime denotes the derivative with respect to τ . The scalar spectral index n_s characterizes the scale dependence of the scalar power spectrum $\mathcal{P}_{\mathcal{R}}(k)$ [31]. With $\frac{z''}{z} \equiv \frac{\nu_R^2 - 1/4}{\tau^2}$,

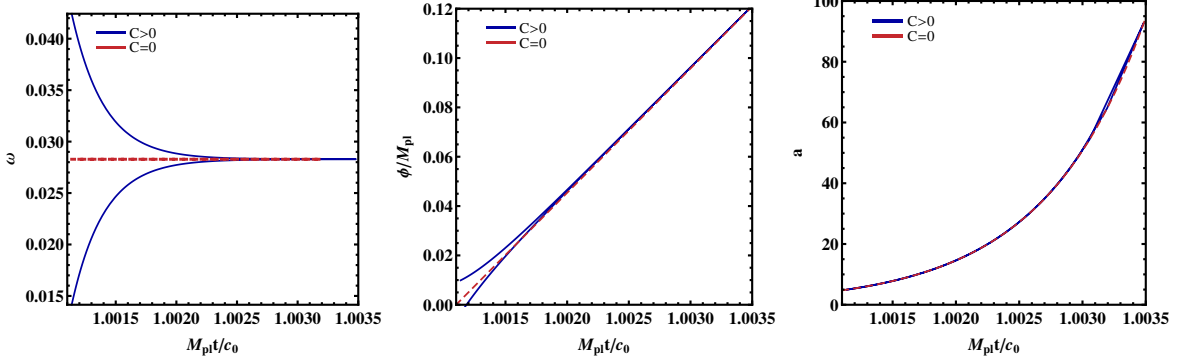


FIG. 2. Numerical solutions of $\omega(t)$, $\phi(t)$, and $a(t)$. The blue curves correspond to the $C > 0$ case, while the red curves represent $C = 0$. The value of λ is fixed to 0.04 because it leads to model parameters that satisfy observational constraints on n_s and r . Different λ values would merely stretch or compress the curves. The horizontal axis $M_{\text{pl}}t/c_0$ is used to remove rescaling caused by C and keeps the time variable dimensionless. For the $C = 0$ case we conventionally set $c_0 = 1$; for the $C > 0$ case, c_0 is defined in Eq. 16, and integration constants are chosen as $t_0 = 0$ and $a_0 = 1$, where t_0 simply sets the horizontal origin without affecting the physical evolution.

n_s can be calculated by

$$n_s - 1 \equiv \frac{d \ln \mathcal{P}_{\mathcal{R}}(k)}{d \ln k} = 3 - 2\nu_R. \quad (29)$$

The validity of Eq. (29) relies on the condition that the quantity $\frac{z''}{z}\tau^2$ remains approximately constant with respect to τ . This approximation will be justified after Eq. (34).

In terms of the slow-roll parameters, the potential in the Mukhanov-Sasaki equation reads [18, 19]

$$\frac{z''}{z} = a^2 H^2 \left(2 + \epsilon_1 + \frac{3}{2}\epsilon_2 + \frac{1}{4}\epsilon_2^2 - \frac{1}{2}\epsilon_1\epsilon_2 + \frac{1}{2}\epsilon_2\epsilon_3 \right), \quad (30)$$

with

$$\epsilon_1 \equiv -\frac{\dot{H}}{H^2} = \omega^2, \quad \epsilon_2 \equiv \frac{\dot{\epsilon}_1}{H\epsilon_1} = -\frac{2}{\omega} (3 - \omega^2) \left(\omega - \frac{\lambda}{\sqrt{2}} \right), \quad (31)$$

$$\epsilon_3 \equiv \frac{\dot{\epsilon}_2}{H\epsilon_2} = 4\omega^2 - 6 + \frac{3\lambda}{\sqrt{2}\omega} (1 - \omega^2), \quad (32)$$

and the conformal time reads

$$\begin{aligned} \tau &= \int_{\infty}^t \frac{1}{a} dt = \int_{\frac{\lambda}{\sqrt{2}}}^{\omega} \frac{1}{a\dot{\phi} \frac{d\omega}{d\phi}} d\omega \\ &= \pm \frac{M_{\text{pl}}\sqrt{C}}{a_0} \int_{\frac{\lambda}{\sqrt{2}}}^{\omega} \left| \sqrt{3} - \omega \right|^{\frac{\sqrt{6}}{3(\sqrt{6}-\lambda)}-1} \times \left| \sqrt{3} + \omega \right|^{\frac{\sqrt{6}}{3(\sqrt{6}+\lambda)}-1} \times \left| \omega - \frac{\lambda}{\sqrt{2}} \right|^{-\frac{4}{6-\lambda^2}} d\omega. \end{aligned} \quad (33)$$

Combining Eqs. (12), (24), (30), and (33), one can find

$$\begin{aligned} \frac{z''}{z} \tau^2 &= \frac{4}{(\lambda^2 - 2)^2 \omega^2} \left(\frac{\sqrt{3} - \frac{\lambda}{\sqrt{2}}}{\sqrt{3} - \omega} \right)^{\frac{2}{3} \frac{\sqrt{6}}{\sqrt{6}-\lambda}} \left(\frac{\sqrt{3} + \frac{\lambda}{\sqrt{2}}}{\sqrt{3} + \omega} \right)^{\frac{2}{3} \frac{\sqrt{6}}{\sqrt{6}+\lambda}} \\ &\times \left[2 \left(\omega - \frac{\lambda}{\sqrt{2}} \right)^2 (9 - 9\omega^2 + 2\omega^4) + \omega^2 (2 + \omega^2) \right] \\ &\times F_1 \left(\frac{2 - \lambda^2}{6 - \lambda^2}; 1 - \frac{1}{3} \frac{\sqrt{6}}{\sqrt{6} - \lambda}, 1 - \frac{1}{3} \frac{\sqrt{6}}{\sqrt{6} + \lambda}; 1 + \frac{2 - \lambda^2}{6 - \lambda^2}; \frac{\omega - \frac{\lambda}{\sqrt{2}}}{\sqrt{3} - \frac{\lambda}{\sqrt{2}}}, -\frac{\omega - \frac{\lambda}{\sqrt{2}}}{\sqrt{3} + \frac{\lambda}{\sqrt{2}}} \right)^2 \end{aligned} \quad (34)$$

Then, the scalar spectral index n_s can be determined with Eqs. (29) and (34).

The quantity $\frac{z''}{z} \tau^2$ must be approximately constant in τ for the slow-roll-like approximation in Eq. (29) to be valid. Since $\frac{z''}{z} \tau^2$ is a function of ω , we analyze its behavior by examining $d\omega/d\tau$ near the stable point $\omega = \lambda/\sqrt{2}$. Following Eq. (33), one has

$$\frac{d\omega}{d\tau} = \left(\frac{d\tau}{d\omega} \right)^{-1} = \pm \frac{a_0}{M_{\text{pl}} \sqrt{C}} \left| \sqrt{3} - \omega \right|^{-\frac{\sqrt{6}}{3(\sqrt{6}-\lambda)}+1} \left| \sqrt{3} + \omega \right|^{-\frac{\sqrt{6}}{3(\sqrt{6}+\lambda)}+1} \left| \omega - \frac{\lambda}{\sqrt{2}} \right|^{\frac{4}{6-\lambda^2}}. \quad (35)$$

Near $\omega \simeq \lambda/\sqrt{2}$ with $|\lambda| < \sqrt{6}$, the above equation implies $d\omega/d\tau \simeq 0$. Thus, ω remains nearly constant without singular behavior. The region $|\lambda| > \sqrt{6}$ is excluded, as it yields values of n_s and r inconsistent with observational constraints.

The evolution of tensor perturbations (or primordial gravity waves) can likewise be formulated [32]. Each Fourier mode of the tensor perturbation, with amplitude u_k , obeys

$$u_k'' + \left(k^2 - \frac{a''}{a} \right) u_k = 0. \quad (36)$$

With $\frac{a''}{a} \equiv \frac{\nu_T^2 - 1/4}{\tau^2}$, the tensor-to-scalar ratio r is given as [33]

$$r \equiv \frac{\mathcal{P}_T}{\mathcal{P}_R} = 16\omega^2 2^{2(\nu_R - \nu_T)} \frac{\Gamma^2(\nu_T)}{\Gamma^2(\nu_R)}, \quad (37)$$

where $\mathcal{P}_T(k)$ is the power spectrum of tensor perturbation, Γ is the Gamma function, and ν_T is given by

$$\nu_T^2 = a^2 H^2 (2 - \omega^2) \tau^2 + \frac{1}{4}. \quad (38)$$

Following the same procedure used to demonstrate the near-constancy of $\frac{z''}{z} \tau^2$, we apply Eqs. (12), (24), and (33) to the tensor spectral index ν_T . This reveals that ν_T likewise remains approximately constant near the stable point $\omega \simeq \lambda/\sqrt{2}$ for $|\lambda| < \sqrt{6}$. Consequently, r can be analytically expressed in terms of ω and λ .

We now examine the evolution of the curvature perturbation ζ on super-horizon scales, where the k^2 term in Eq. (28) becomes negligible. The general solution of ζ is given by

$$\zeta_k(\tau) = A_k + B_k \int^{\tau} \frac{1}{z^2(\bar{\tau})} d\bar{\tau}, \quad (39)$$

with integration constants A_k and B_k . The conservation of ζ depends critically on whether the integral term converges to a constant value as the system approaches the stable point. Since the integral is monotonically increasing, if it converges to a constant, this constant can be absorbed into A_k , yielding a decaying mode (a negative, increasing function). Otherwise, the integral corresponds a growing mode. Changing the integral variable to ω , the integral becomes

$$\int^{\tau} \frac{1}{z^2(\tau)} d\tau = \int^{\omega} \frac{1}{z^2} \frac{d\tau}{d\omega} d\omega = \frac{1}{2M_{\text{pl}}^2} \int^t \frac{1}{a^3 \omega^2} dt = \frac{1}{2M_{\text{pl}}^2} \int^{\omega} \frac{1}{a^3 \omega^2} \frac{1}{\frac{d\omega}{d\phi}} d\omega. \quad (40)$$

Using Eq. (24), one can find

$$\int^{\tau} \frac{1}{z^2(\tau)} d\tau \sim \int^{\omega} \frac{1}{\omega^2 (3 - \omega^2)} d\omega. \quad (41)$$

From earlier stability discussion, the integral diverges at the stable point $\omega = 0$ and $\omega = \pm\sqrt{3}$, while it converges at $\omega = \frac{\lambda}{\sqrt{2}}$. Therefore, the only physical solution is the mode evolving toward $\omega = \frac{\lambda}{\sqrt{2}}$, in which the curvature perturbation is conserved on super-horizon scales.

Using Eqs. (29) and (37), the scalar spectral index and the tensor-to-scalar ratio for different values of ω and λ are calculated. Figure 3 compares these calculations with the most recent observational constraints from Planck 2018 data ($n_s = 0.9649 \pm 0.0042$ [20]) and a combination of BICEP/Keck 2018 and Planck PR4 data ($r < 0.032$ at 95% C.L. [21–23]). This demonstrates that there exists a parameter space that satisfies the observational constraints. The apparent double-valued behavior for $C > 0$ arises because n_s is a complicated, non-monotonic function of ω . Different values of ω may correspond to the same n_s . Each branch corresponds to a different ω , and within the current theoretical framework there is no strong reason to prefer one branch over the other. The choice of branch would ultimately depend on more precise future observational constraints.

The observational constraints on n_s and r impose tight restrictions on the model parameters, often requiring high-precision tuning. For example, a finely tuned parameter set $(\lambda, \omega) = (0.040 \pm 0.001, 0.027 \pm 0.001)$ yields $(n_s, r) = (0.9700 \pm 0.0064, 0.012 \pm 0.001)$, where

the uncertainty of n_s is already larger than that of experimental measurements. Around this parameter space, we derive an approximate expression for the number of e-foldings, and subsequently demonstrate that ω represents an attractor solution, although it has been implicitly defined in Eq. (13). Assuming the stable point is $\omega = \frac{\lambda}{\sqrt{2}}$, the range of values for w during inflation is between $[0.027, \frac{0.040}{\sqrt{2}}]$, which leads to

$$\frac{\omega_e}{\omega} \sim \mathcal{O}(1), \quad \frac{\sqrt{3} \pm \omega_e}{\sqrt{3} \pm \omega} \sim \mathcal{O}(1). \quad (42)$$

Consequently, the e-foldings in Eq. (23) is approximated to be

$$N_e - N \simeq \frac{2}{6 - \lambda^2} \ln \left| \frac{\omega - \frac{\lambda}{\sqrt{2}}}{\omega_e - \frac{\lambda}{\sqrt{2}}} \right|. \quad (43)$$

In typical studies, the behavior of δH is examined to determine whether the solution is an attractor, but this approach is not convenient in this work. The δw is instead analyzed. According to Eq. (12), δw decreases synchronously with δH , making ω an equally valid indicator of attractor behavior.

From the equation of motion, Eq. (13), one can derive the differential relation for ω :

$$\frac{d\delta\omega}{\delta\omega} = \left(\frac{1}{\omega - \frac{\lambda}{\sqrt{2}}} - \frac{2\omega}{3 - \omega^2} - \frac{1}{\omega} \right) d\omega, \quad (44)$$

Solving the above equation yields the evolution of ω

$$\begin{aligned} \delta\omega_e &= \delta\omega \frac{3 - \omega_e^2}{3 - \omega^2} \left| \frac{\omega}{\omega_e} \right| \times \left| \frac{\omega - \frac{\lambda}{\sqrt{2}}}{\omega_e - \frac{\lambda}{\sqrt{2}}} \right| \\ &\simeq \delta\omega \exp \left[-\frac{6 - \lambda^2}{2} (N_e - N) \right] \simeq \delta\omega \exp [-3(N_e - N)] \end{aligned} \quad (45)$$

Based on the results, the evolution of w , which satisfies the constraints on n_s and r , represents an attractor solution. Specifically, w asymptotically approaches the attractor point $\omega = \frac{\lambda}{\sqrt{2}}$. This reveals that both the general solutions presented in our work and the particular solutions ($\omega = \frac{\lambda}{\sqrt{2}}$) discussed in previous studies belong to the same class of attractors. It is important to emphasize that the attractor solution in this case should be understood as a family of solutions rather than a single, isolated trajectory: as the independent variable evolves, different solutions within this family approach each other asymptotically [11].

In summary, despite its simplicity and elegance, power-law inflation was considered excluded due to the failure of its particular solution to match observations. We have derived

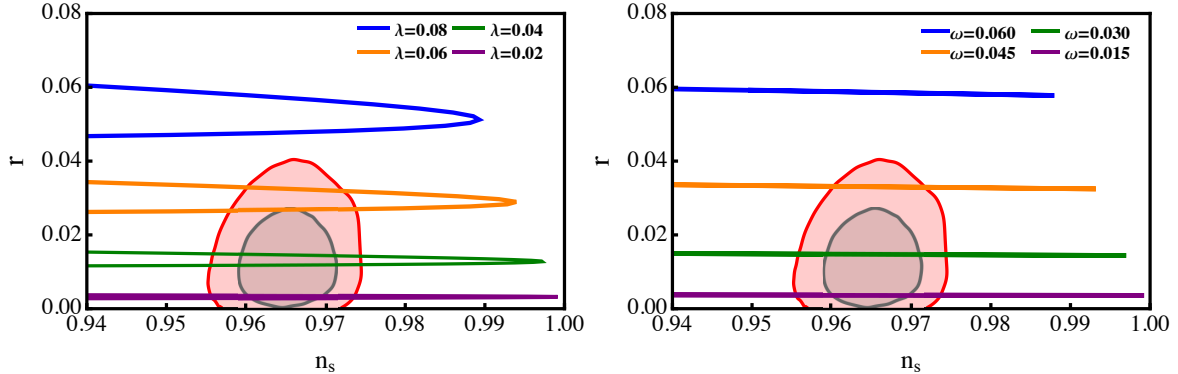


FIG. 3. Parameter space consistent with the current constraints on n_s and r , as inferred from Planck 2018 data [20] and a combination of BICEP/Keck 2018 and Planck PR4 data [21–23]. The solid contours indicate the 68% (1σ) and 95% (2σ) confidence levels.

the general solutions of power-law inflation analytically and demonstrated that power-law inflation is still valid.

The particular solution corresponds to the trajectory where ω always equal to $\frac{\lambda}{\sqrt{2}}$, while the general solutions corresponds to the different trajectories approaching $\omega = \frac{\lambda}{\sqrt{2}}$. Since the scalar spectral index and tensor-to-scalar ratio are not only dependent on the attractor itself, but also highly sensitive to the trajectories how to approach the stable point. It is logically flawed to exclude a potential model solely based on one trajectory of the attractor solution that does not meet these constraints. We have proved some of the trajectories from the general solutions of power-law inflation can satisfy the observational constraints.

Moreover, power-law inflation can also be analyzed using the slow-roll approximation [34]. These approximate results are consistent with those obtained from the exact particular solution [35], but both approaches do not agree with experimental observations. Our work demonstrates that the slow-roll approximation may fail in certain cases. Similar issues have been studied in the context of ultra slow-roll models [36], where the slow-roll approximation may also break down.

Finally, our model provides an example showing that certain inflationary scenarios, previously ruled out under the slow-roll approximation, may in fact possess viable parameter space with more accurate calculations.

ACKNOWLEDGMENTS

The authors gratefully acknowledge Dr. Wei Cheng and Dr. Ruiyu Zhou for their insightful discussions and valuable feedback. Yao Yu, Wen-Zhang Feng and Hong-Song Xie were supported in part by NSFC under Contracts No. 11905023, No. 12047564 and No. 12147102, the Natural Science Foundation of Chongqing (CQCSTC) under Contract No. cstc2020jcyj-msxmX0555, and the Science and Technology Research Program of Chongqing Municipal Education Commission (STRPCMEC) under Contracts No. KJQN202200605 and No. KJQN202200621; Han Zhang and Bai-Cian Ke were supported in part by National Natural Science Foundation of China (NSFC) under Contracts No. 12192263, Joint Large-Scale Scientific Facility Fund of the NSFC and the Chinese Academy of Sciences under Contract No. U2032104, and the Excellent Youth Foundation of Henan Scientific Committee under Contract No. 242300421044.

-
- [1] A. H. Guth, *Phys. Rev. D* **23**, 347-356 (1981) doi:10.1103/PhysRevD.23.347
 - [2] A. A. Starobinsky, *Phys. Lett. B* **91**, 99-102 (1980) doi:10.1016/0370-2693(80)90670-X
 - [3] A. D. Linde, *Phys. Lett. B* **129**, 177-181 (1983) doi:10.1016/0370-2693(83)90837-7
 - [4] A. A. Starobinsky, *JETP Lett.* **30**, 682-685 (1979)
 - [5] V. F. Mukhanov and G. V. Chibisov, *JETP Lett.* **33**, 532-535 (1981)
 - [6] L. F. Abbott and M. B. Wise, *Nucl. Phys. B* **244**, 541-548 (1984) doi:10.1016/0550-3213(84)90329-8
 - [7] F. Lucchin and S. Matarrese, *Phys. Rev. D* **32**, 1316 (1985) doi:10.1103/PhysRevD.32.1316
 - [8] V. Sahni, *Class. Quant. Grav.* **5**, L113 (1988) doi:10.1088/0264-9381/5/7/002
 - [9] B. Ratra, *Phys. Rev. D* **40**, 3939 (1989) doi:10.1103/PhysRevD.40.3939
 - [10] B. Ratra, *Phys. Rev. D* **45**, 1913-1952 (1992) doi:10.1103/PhysRevD.45.1913
 - [11] A. R. Liddle, P. Parsons and J. D. Barrow, *Phys. Rev. D* **50**, 7222-7232 (1994) doi:10.1103/PhysRevD.50.7222 [arXiv:astro-ph/9408015 [astro-ph]].
 - [12] G. Domènech, G. Vargas and T. Vargas, *JCAP* **03**, 002 (2024) doi:10.1088/1475-7516/2024/03/002 [arXiv:2309.05750 [astro-ph.CO]].

- [13] E. Kamke, *Differentialgleichungen: Lösungsmethoden und Lösungen I: Gewöhnliche Differentialgleichungen*, 9th ed., with a preface by Detlef Kamke, B.G. Teubner, Stuttgart, Germany, 1977.
- [14] A.D. Polyanin and V.F. Zaitsev, *Handbook of Exact Solutions for Ordinary Differential Equations*, 2nd ed., Chapman and Hall/CRC, Boca Raton, 2003.
- [15] A. G. Muslimov, *Class. Quant. Grav.* **7** (1990), 231-237 doi:10.1088/0264-9381/7/2/015
- [16] A. V. Yurov and V. A. Yurov, *J. Math. Phys.* **51**, 082503 (2010) doi:10.1063/1.3460856 [arXiv:0809.1216 [hep-th]].
- [17] P. Christodoulidis, *Eur. Phys. J. C* **81**, no.5, 471 (2021) doi:10.1140/epjc/s10052-021-09268-5 [arXiv:1811.06456 [astro-ph.CO]].
- [18] M. B. Hoffman and M. S. Turner, *Phys. Rev. D* **64** (2001), 023506 doi:10.1103/PhysRevD.64.023506 [arXiv:astro-ph/0006321 [astro-ph]].
- [19] D. J. Schwarz, C. A. Terrero-Escalante and A. A. Garcia, *Phys. Lett. B* **517** (2001), 243-249 doi:10.1016/S0370-2693(01)01036-X [arXiv:astro-ph/0106020 [astro-ph]].
- [20] Y. Akrami et al. [Planck], *Planck 2018 results. X. Constraints on inflation*, *Astron. Astrophys.* **641**, A10 (2020) doi:10.1051/0004-6361/201833887 [arXiv:1807.06211 [astro-ph.CO]].
- [21] M. Tristram, A. J. Banday, K. M. Górski, R. Keskitalo, C. R. Lawrence, K. J. Andersen, R. B. Barreiro, J. Borrill, L. P. L. Colombo and H. K. Eriksen, *et al.* *Phys. Rev. D* **105**, 083524 (2022) doi:10.1103/PhysRevD.105.083524 [arXiv:2112.07961 [astro-ph.CO]].
- [22] M. Tristram, A. J. Banday, K. M. Górski, R. Keskitalo, C. R. Lawrence, K. J. Andersen, R. B. Barreiro, J. Borrill, H. K. Eriksen and R. Fernandez-Cobos, *et al.* *Astron. Astrophys.* **647**, A128 (2021) doi:10.1051/0004-6361/202039585 [arXiv:2010.01139 [astro-ph.CO]].
- [23] P. A. R. Ade *et al.* [BICEP and Keck], *Phys. Rev. Lett.* **127**, no.15, 151301 (2021) doi:10.1103/PhysRevLett.127.151301 [arXiv:2110.00483 [astro-ph.CO]].
- [24] T. H. Koornwinder and J. V. Stokman (Eds.), *Encyclopedia of Special Functions: The Askey-Bateman Project*, Cambridge University Press, Cambridge, 2020.
- [25] Wikipedia contributors, *Appell series*, *Wikipedia, The Free Encyclopedia*, 2026, https://en.wikipedia.org/wiki/Appell_series.
- [26] H. Motohashi, A. A. Starobinsky and J. Yokoyama, *JCAP* **09**, 018 (2015) doi:10.1088/1475-7516/2015/09/018 [arXiv:1411.5021 [astro-ph.CO]].

- [27] H. Motohashi and A. A. Starobinsky, EPL **117**, no.3, 39001 (2017) doi:10.1209/0295-5075/117/39001 [arXiv:1702.05847 [astro-ph.CO]].
- [28] A. D. Linde, Phys. Rev. D **49**, 748-754 (1994) doi:10.1103/PhysRevD.49.748 [arXiv:astro-ph/9307002 [astro-ph]].
- [29] V. F. Mukhanov, JETP Lett. **41**, 493-496 (1985)
- [30] M. Sasaki, Prog. Theor. Phys. **76**, 1036 (1986) doi:10.1143/PTP.76.1036
- [31] E. D. Stewart and D. H. Lyth, Phys. Lett. B **302**, 171-175 (1993) doi:10.1016/0370-2693(93)90379-V [arXiv:gr-qc/9302019 [gr-qc]].
- [32] V. F. Mukhanov, H. A. Feldman and R. H. Brandenberger, Phys. Rept. **215**, 203-333 (1992) doi:10.1016/0370-1573(92)90044-Z
- [33] J. E. Lidsey, A. R. Liddle, E. W. Kolb, E. J. Copeland, T. Barreiro and M. Abney, Rev. Mod. Phys. **69**, 373-410 (1997) doi:10.1103/RevModPhys.69.373 [arXiv:astro-ph/9508078 [astro-ph]].
- [34] A. R. Liddle and D. H. Lyth, Cosmological inflation and large-scale structure. Cambridge university press, 2000. doi:10.1017/CBO9781139175180
- [35] S. Weinberg, Cosmology. Oxford University Press, 2008
- [36] K. Dimopoulos, Phys. Lett. B **775** (2017), 262-265 doi:10.1016/j.physletb.2017.10.066 [arXiv:1707.05644 [hep-ph]].